

ELECTRONIC SUPPLEMENTARY INFORMATION

ICPF 1D MODEL

In order to extract the analytes, the focused analyte peaks must be precisely placed at the location where the extraction channels intersect the sample channel. Since different analytes are focused in different locations in the E-field gradient, the gradient needs to be moved so that the concentrated band of the analyte of interest overlaps with the location of the extraction channel and it can be selectively extracted. In order to change the position of the E-field gradient we need to regulate the length of depletion zone (dz).

The length of the dz , l^u , can be regulated by two phenomena that have an opposite effect, namely ICP and the linear convective flow which is dominated by EOF. Both phenomena are driven by an E-field; ICP by the E-field across the Nafion membrane and EOF by the E-field between up- and downstream reservoirs. The EOF velocity scales linearly with the potential difference between up- and downstream reservoirs as shown in Helmholtz-Smoluchowski equation (equation (5) of the main article). In this way the electric and the fluidic model are coupled. The simulation is performed in incremental time steps. For each time step the

electric model calculates the expansion of dz due to ICP ($\frac{dl_e}{dt}$ equation 2 of the article). The volumetric flow and linear flow velocity ($\frac{dl_f}{dt}$) are then calculated by the fluidic model and fed back to the electric model.

As described in literature[1] and as also follows from our model, the length of dz due to ICP under a no-flow condition (no EOF or PDF, $V^u = V^d, \frac{dl_f}{dt} = 0$), grows with the square root of time under constant voltage actuation (Figure 1).

$$l^u = -l^d = \beta t^{1/2}$$

$$\frac{dl^u}{dt} = \frac{1}{2} \beta t^{-1/2}$$

The scaling factor β depends on various parameters of the system, i.e. applied potentials, channel dimensions, Nafion properties, bulk and depletion zone conductivity, bulk and depletion zone concentrations.

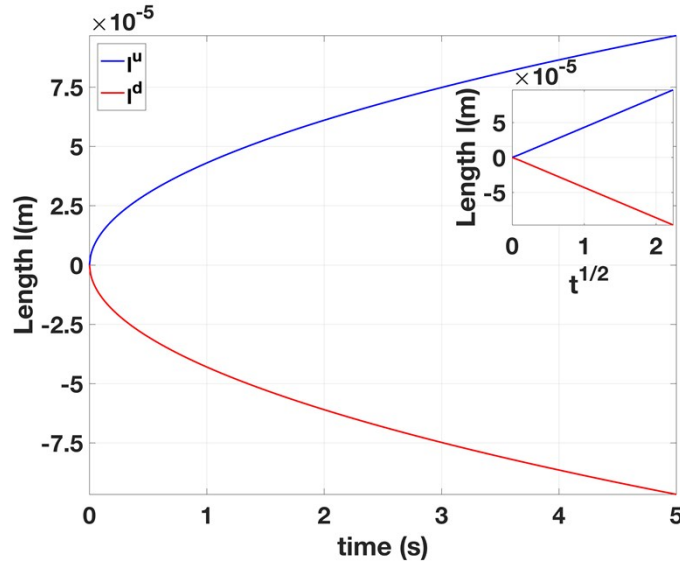


Figure 1- Depletion zone length upstream (l^u) and downstream (l^d) vs time under no convective flow condition ($V^u = V^d = 30V$) following from the model. The expected square root of time behavior can be seen.

When EOF from upstream to downstream reservoir ($V^u > V^d$) is introduced, upstream from the Nafion the flow opposes the growth of dz and $\frac{dl_f}{dt}$, $\frac{dl_e}{dt}$ are opposite and the iteration process will result in a stable depletion zone length (l^u). In contrast, downstream from the Nafion $\frac{dl_f}{dt}$ and $\frac{dl_e}{dt}$ have the same sign and the depletion zone (l^d) will grow until the downstream reservoir is reached. The focusing position depends on l^u (i.e. scaling factor β) and the zeta potential in the bulk and the depletion zone.

The focusing position of the analytes can be regulated by adjusting the reservoir potentials. As shown in figure 2 the smaller the difference between upstream and downstream potential the further away the stable focusing position will become located from the Nafion interface. If the reservoir potentials are changed in magnitude but the ratio between both remains constant, then the focusing position is constant. In contrast the concentration rate and the induced pressure scale directly with the magnitude of the applied potential difference between upstream and downstream (Figure 3,4). A typical approach to increase the preconcentration rate in standard ICPF devices is to apply an extra PDF between the upstream and downstream reservoir[2]. This behavior can also be described by our model by applying the corresponding potentials (pressures) on the now grounded reservoir nodes of the fluidic model. Though the model can describe the general behaviour of the system, exact prediction is a challenging process since some parameters of the system are unknown. Specifically, the concentration, conductivity and zeta potential in the depletion zone are unknown. We used an estimate of the concentration based on experimental results of similar devices. Kim et al[4] report a 33-fold increase in the E-field in the depletion zone compared to bulk E-field, which translates to a 33-fold decreased conductivity in the depletion zone compared to the bulk buffer (1mM phosphate (dibasic sodium phosphate)). Nevertheless, in depletion zone systems electroconvective vortices enhance the conductivity in the depletion zone by introducing extra charge carriers[3], [4] hence only an approximation of the average concentration can be obtained from the conductivity. The low salt concentration in the depletion zone is expected also to locally increase the zeta potential. The zeta potential is also

greatly influenced by the pH[5], [6] which is reported[7] to be more acidic close to the depletion zone. Finally, our model neglects the effect of diffusion between bulk and depletion zone.

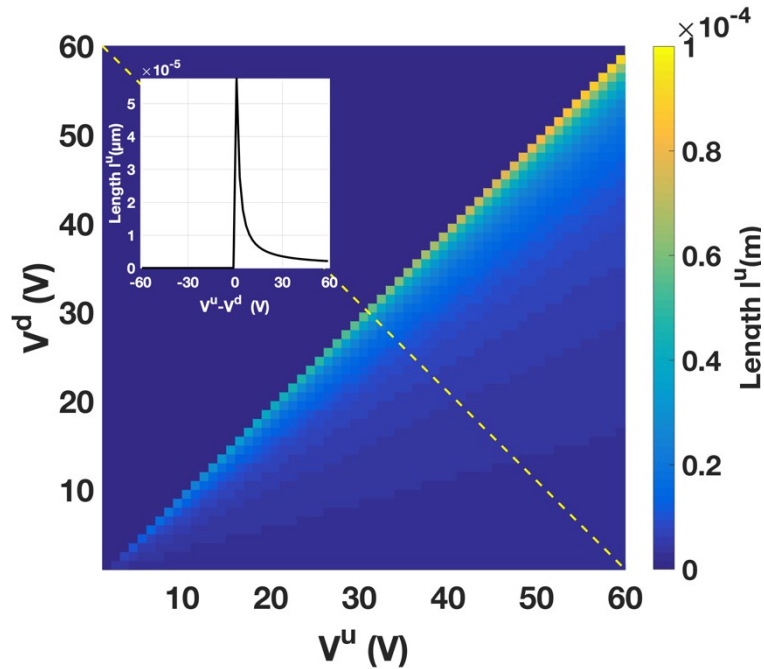


Figure 2- Focusing position (l^u) shown in color map (as distance from Nafion in meters) vs actuation potentials (V^u, V^d) at $t=5s$ (Note: the position is constant over time after $t\sim 3s$). The smaller the potential difference, the further the focusing position from the Nafion (i.e. the bigger the depletion zone). The response of the focusing position versus potential difference is shown in the inset figure. In case that the $V^u < V^d$ the depletion zone will reach a stable size towards the downstream reservoir and it will grow all the way to upstream reservoir. If the ratio between potentials is kept constant, a constant focusing position is achieved.

The preconcentration rate describes the local increase of concentration of analyte over time and is expressed as the number of times increase of the analyte relative to its starting/bulk concentration per unit of time. We assume all the anions that arrive at the interface between depletion zone are focused as described in the main article, hence the preconcentration rate simply scales with the flux (J_i) of each species in the separation channel arriving to the depletion zone.

$$J_i = v_{conv} C_i^b$$

Here v_{conv} is the convective flow and C_i^b is the bulk concentration of species i . The preconcentration rate thus simply scales with the bulk volumetric flow, as bulk flow brings analytes to their focusing position in the E-field gradient between bulk liquid and depletion zone. The higher the flow, the higher the number of analytes arriving at the location at the E-field gradient where they have zero-net velocity, and the highest the preconcentration rate.

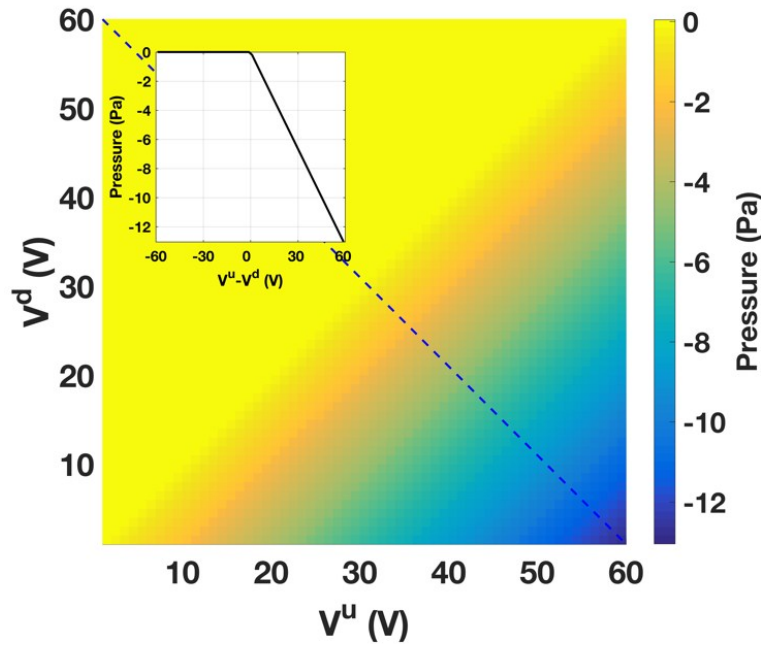


Figure 3- Induced negative pressure vs actuation potentials (V^u, V^d) at $t=5\text{sec}$. The induced pressure scales linearly with the potential difference between V^u and V^d as shown by the inset figure.

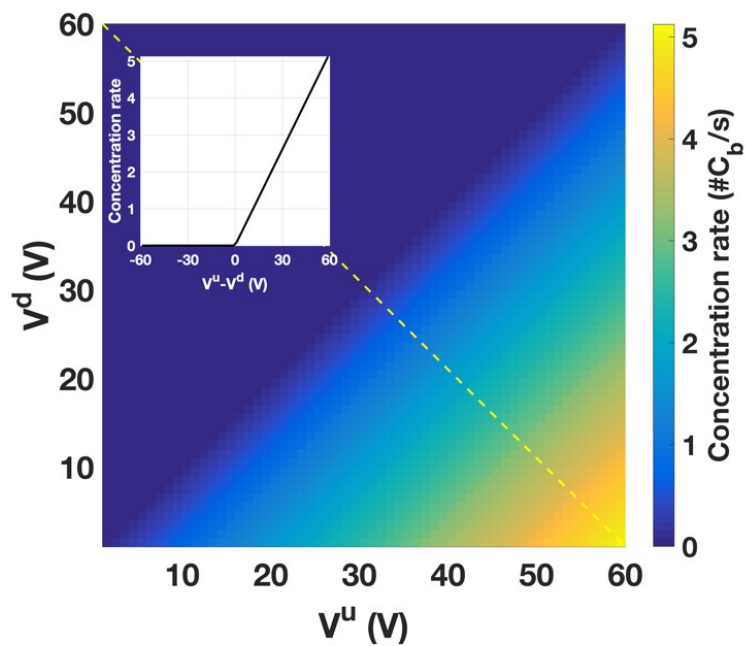


Figure 4- Preconcentration rate (number of times the bulk concentration (C_b) per second) vs actuation potentials (V^u, V^d) at $t=5\text{sec}$ assuming a focused analyte plug of $125\mu\text{m}$ in width. The preconcentration rate scales approximately linearly with the potential difference between V^u and V^d as shown by the inset figure.

Derivation of focused analyte peak size and distribution

We will follow the approach of J.C. Gidding[8] for focusing techniques. Neglecting the incoming flux of analyte, the peak profile follows from the opposing electrical and diffusional fluxes. For steady state we can write:

$$J_{i,0} = v_i C_i(x) - D_i \frac{dC_i}{dx} = 0 \quad (1)$$

Here v_i is the linear analyte velocity, C_i is concentration and D_i the diffusion coefficient of species i . From this we can write the differential equation

$$\frac{1}{C_i} \frac{dC_i}{dx} = \frac{v_i(x)}{D_i} \quad (2)$$

The velocity v_i of anion i equals

$$v_i(x) = v_{conv} + v_{eph}(x)$$

$$v_i(x) = v_{conv} - \mu_i E(x) = v_{conv} - \mu_i \left(E_0 + \frac{dE}{dx} x \right) \quad (3)$$

Here E_0 is the electric field in the bulk and μ_i the electrophoretic mobility. Substitution in equation (1) gives

$$\frac{1}{C_i} \frac{dC_i}{dx} = \frac{v_{conv} - \mu_i \left(E_0 + \frac{dE}{dx} x \right)}{D_i} \quad (4)$$

From this we can write the integral

$$\int_{C_{i,0}}^{C_{i,x}} \frac{1}{C_i} dC_i = \int_0^x \frac{v_{conv} - \mu_i \left(E_0 + \frac{dE}{dx} x \right)}{D_i} dx \quad (5)$$

Assuming a constant E-field gradient $\frac{dE}{dx}$ we obtain

$$\ln \left(\frac{C_{i,x}}{C_{i,0}} \right) = \frac{(v_{conv} - \mu_i E_0)x - \frac{1}{2} \frac{dE}{dx} \mu_i x^2 + \beta}{D_i} \quad (6)$$

We thus obtain the expression for the concentration profile of an analyte in peak mode,

$$C_i(x) = C_{i,0} \exp \left(\frac{(v_{conv} - \mu_i E_0)x - \frac{1}{2} \frac{dE}{dx} \mu_i x^2 + \beta}{D_i} \right) \quad (7)$$

The constant β can be calculated via the known value of $C_i(x_{eq}) = C_{i,0}$. The focusing position x_{eq} where the electrophoretic and convective flow are equal and opposite, and where the anion has zero net velocity (i.e. where Equation 3 equals to 0) is

$$x_{eq,i} = \frac{v_{conv} - E_0\mu_i}{\frac{dE}{dx}\mu_i} \quad (8)$$

The focusing location x_{eq} is shown in figure 7 as a function of electrophoretic mobility for a typical actuation potential ($V^u - V^d = 60V$).

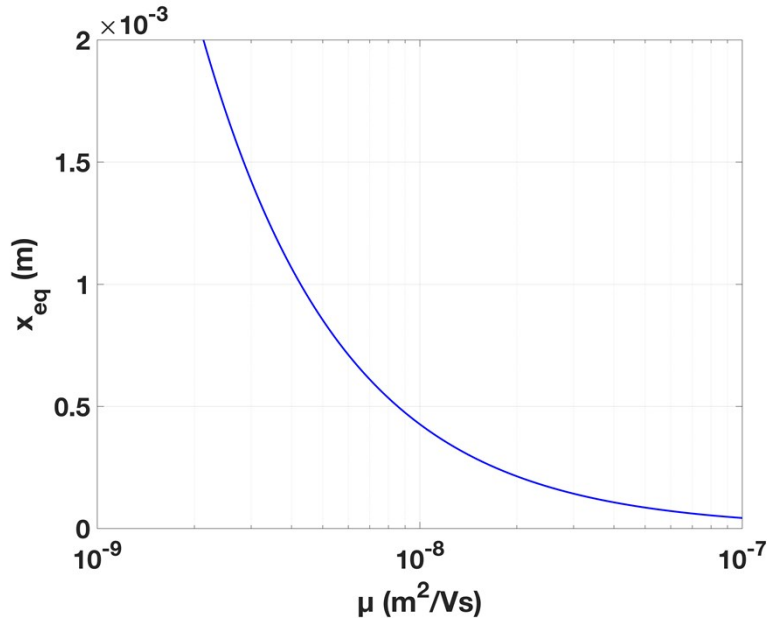


Figure 5 – Focusing location vs electrophoretic mobility.

After calculating β we can rewrite equation 7 in its final form:

$$C_i(x) = C_{i,0} \exp \left(- \frac{\left(x - \frac{v_{conv} - E_0\mu_i}{\frac{dE}{dx}\mu_i} \right)^2}{\frac{D_i}{2 \frac{dE}{dx} \mu_i}} \right) \quad (9)$$

Equation 9 describes a Gaussian distribution with a mean equal to x_{eq} (Equation 8). At x_{eq} the analyte will focus and create a Gaussian peak with a variance of

$$\sigma^2 = \frac{D_i}{\frac{dE}{dx} \mu_i} \quad (10)$$

Since the diffusion coefficients and electrophoretic mobilities are related via Einstein's relation,

$$D_i = \frac{k_b T}{q_i} \mu_i = \frac{V_T}{z_i} \mu_i \quad (11)$$

(with k_b is the Boltzmann constant, T the temperature, V_T the thermal voltage and z_i the valence of the ion), we can rewrite the variance in a simpler form,

$$\sigma^2 = \frac{V_T}{\frac{dE}{z_i dx}} \quad (12)$$

Equation 12 might appear counterintuitive since it is independent of electrophoretic mobility and diffusion coefficient of a specific analyte, but since at the focusing location the ion has zero net velocity any size-dependent variables drop out. Simply put, the ionic thermal energy (V_T) increases the variance while the electric field gradient reduces it.

Resolution

As shown in equation 12 of the main article the resolution of the separation method equals to:

$$R_s = \frac{v_{conv}}{2 \sqrt{\frac{dE}{dx} V_T}} \cdot \frac{\left(\frac{1}{\mu_1} - \frac{1}{\mu_2} \right)}{\left(\frac{1}{\sqrt{z_1}} + \frac{1}{\sqrt{z_2}} \right)} \quad (16)$$

Our model allow us to calculate the total convective flow in the separation channel along with the electric field in the bulk (E_B) and depletion zone (E_{dz}) and the electric field difference ($\Delta E = E_{dz} - E_B$). One still unknown variable is the size of the concentration gradient between bulk and depletion zone (electric field gradient size). According to Mani et al.[9] the size of such gradient (l_{grad}) scales with the average diffusion coefficient (D) and the characteristic velocity of the system in our case the convective velocity.

$$l_{grad} \sim \frac{D}{v_{conv}} \quad (17)$$

Intuitively equation 17 describes that diffusion acts towards a flatter gradient while the opposing flow act towards a steeper gradient assuming constant concentration in the depletion zone and in the bulk. Using equation 17 and assuming a constant electric field gradient we can write

$$\frac{dE}{dx} = \frac{\Delta E}{l_{grad}} \quad (18)$$

On figure 6 the resolution for separation of Bodipy ($\mu_{BDP} = 1.76 \cdot 10^{-8} \text{ m}^2 \text{V}^{-1} \text{s}^{-1}$) and Alexa fluor 647 ($\mu_{AF647} = 1.58 \cdot 10^{-8} \text{ m}^2 \text{V}^{-1} \text{s}^{-1}$). As it can be seen for low potential difference the resolution is drastically improved compared to high potential difference where poor and constant resolution can be seen. Nevertheless, the improved resolution comes at a cost of concentration rate since as it shown on figure 4 the lower the potential difference the lower the concentration rate.

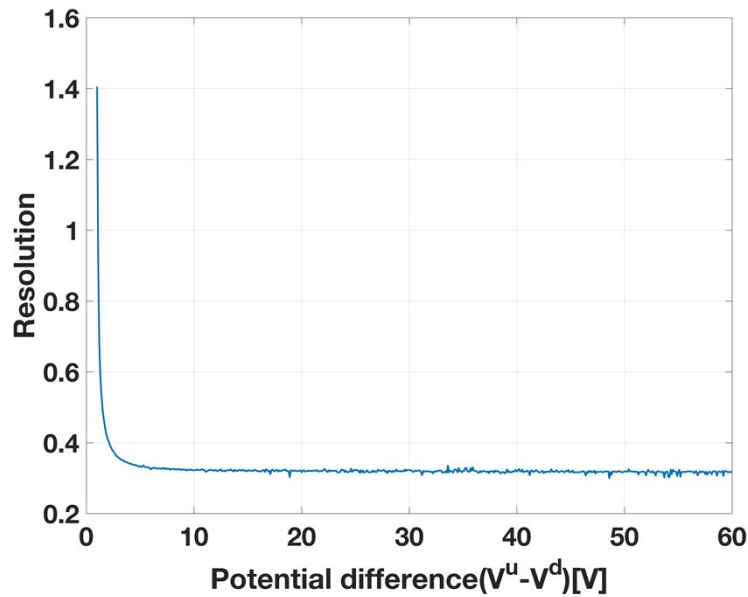


Figure 6 – Resolution vs potential difference ($V^u = 60V$, and V^d ranged from 0 to 59V)

References

- [1] T. A. Zangle, A. Mani, and J. G. Santiago, "Effects of constant voltage on time evolution of propagating concentration polarization," *Anal. Chem.*, vol. 82, no. 8, pp. 3114–3117, 2010.
- [2] J. K. Sung and J. Han, "Self-sealed vertical polymeric nanoporous-junctions for high-throughput nanofluidic applications," *Anal. Chem.*, vol. 80, no. 9, pp. 3507–3511, 2008.
- [3] J. C. De Valena, R. M. Wagterveld, R. G. H. Lammertink, and P. A. Tsai, "Dynamics of microvortices induced by ion concentration polarization," *Phys. Rev. E - Stat. Nonlinear, Soft Matter Phys.*, vol. 92, no. 3, 2015.
- [4] S. J. Kim, Y. C. Wang, J. H. Lee, H. Jang, and J. Han, "Concentration polarization and nonlinear electrokinetic flow near a nanofluidic channel," *Phys. Rev. Lett.*, vol. 99, no. 4, 2007.
- [5] B. J. Kirby and E. F. Hasselbrink, "Zeta potential of microfluidic substrates: 1. Theory, experimental techniques, and effects on separations," *Electrophoresis*, vol. 25, no. 2, pp. 187–202, 2004.
- [6] B. J. Kirby and E. F. Hasselbrink, "Zeta potential of microfluidic substrates: 2. Data for polymers," *Electrophoresis*, vol. 25, no. 2, pp. 203–213, 2004.
- [7] K. Mogi, "A visualization technique of a unique pH distribution around an ion depletion zone in a microchannel by using a dual-excitation ratiometric method," *Micromachines*, vol. 9, no. 4, 2018.
- [8] J. C. Giddings, *Unified Separation Science*. John Wiley & Sons, 1991.
- [9] A. Mani, T. A. Zangle, and J. G. Santiago, "On the propagation of concentration polarization from microchannel - nanochannel interfaces Part I: Analytical model and characteristic analysis," *Langmuir*, vol. 25, no. 6, pp. 3898–3908, 2009.